processes

MDPI

Article

Assessment of PCDD/Fs Emission during Industrial-Organic-Solid-Waste Incineration Process in a Fluidized-Bed Incinerator

Yuxuan Ying [1], Xiaoxiao Wang [1], Wenlong Song [1], Yunfeng Ma [1], Hong Yu [1], Xiaoqing Lin [1,*], Shengyong Lu [1], Xiaodong Li [1], Wei Huang [2] and Li Zhong [3]

[1] State Key Laboratory for Clean Energy Utilization, Institute for Thermal Power Engineering, Zhejiang University, Hangzhou 310027, China
[2] Nanjing Power Plant, Huaneng Power International Jiangsu Energy Development Co., Ltd., Nanjing 210035, China
[3] Beijing Huaneng Yangtze Environmental Technology Research Institute Co., Ltd., Beijing 102209, China
* Correspondence: linxiaoqing@zju.edu.cn; Tel.: +86-0571-87951950

Abstract: This study was conducted in a fluidized-bed incineration plant, evaluating the formation, emission and flux of polychlorinated dibenzo-*p*-dioxins and dibenzofurans (PCDD/Fs) from industrial-organic-solid-waste (IW) incineration. The results revealed that both the total (or I-TEQ) concentrations of toxic and 136 total PCDD/Fs in flue gas (FG), fly ash (FA) and bottom ash (BA)were ramped up to a higher level than those during municipal-solid-waste (MSW) incineration. A possible explanation was the chlorine (Cl) content of IW. However, the emitted PCDD/Fs in FG (FA/BA) still fulfilled the criteria. Subsequently, similar distribution patterns of PCDD/F isomers were observed in subsystems, indicating a unified formation-pathway. De novo synthesis was detected as the dominant formation-pathway of PCDD/Fs, while high-temperature and precursor syntheses were excluded. DD/DF chlorination formed PCDD/Fs to some extent. Furthermore, the mass flow chart indicated that PCDD/Fs output in primary FG was significantly strengthened (>1000 times) by de novo synthesis, from 1.25 µg I-TEQ/h to 1.67 mg I-TEQ/h. With effective cleaning by APCS, 99.6% of PCDD/Fs in FG were purified. PCDD/Fs in the gas phase were finally emitted at a discharge rate of 7.25 µg I-TEQ/h. However, accumulated FA took most PCDD/Fs into the environment (>99%), reaching 3.56 mg I-TEQ/h.

Keywords: flue gas; fly ash; dioxins; incineration; industrial waste; emission characteristic

Citation: Ying, Y.; Wang, X.; Song, W.; Ma, Y.; Yu, H.; Lin, X.; Lu, S.; Li, X.; Huang, W.; Zhong, L. Assessment of PCDD/Fs Emission during Industrial-Organic-Solid-Waste Incineration Process in a Fluidized-Bed Incinerator. *Processes* **2023**, *11*, 251. https://doi.org/10.3390/pr11010251

Academic Editor: Aldo Muntoni

Received: 15 December 2022
Revised: 6 January 2023
Accepted: 9 January 2023
Published: 12 January 2023

1. Introduction

It is widely accepted that the municipal-solid-waste (MSW) output has had a steady increase in the past decade, reaching 0.24 billion t/year by 2020 in China [1]. Likewise, the industrial-waste (IW) generation in China rose from 2.41 billion t/year [2] to 3.67 billion t/year [1] (2010 to 2020). Approximately 55.4% of generated IW was comprehensively utilized in China in 2020 [1], while a considerable amount of IW was directly dumped and discarded (1.13 million t/year in 2020), indicating that further improvement of IW disposal was urgently needed [3]. If not collected, transported, preserved and treated properly, IW would pose a continuous threat to the national public health, and raise social concerns. Industrial waste from different sources varies significantly in its physicochemical characteristics, such as bio-toxicity, flammability, active/inert reactivity and corrosivity [4]. Major IW is divided into inorganic/organic types (80/20 wt%). Inorganic IW includes refining ash, steel slag, coal ash, etc., and organic IW includes leather, textile, papermaking waste and food-industry byproducts [5]. Inorganic IW is mostly composed of salts, is thus non-combustible, and is disposed by mature technologies such as solidification and landfill [6]. However, organic IW disposal still lacks universal treatment approaches, due to its heterogeneous components. Possibly, organic IW is able to be treated through incineration, bio-composting, microwave disintegration and co-combustion [7,8].

Leather waste, as a kind of typical organic IW produced by the tanning industry, was exceedingly difficult to handle. It also contributed an enormous quantity of more than 200 million t/year in China (ranked first all over the world) [9]. The primary materials of leather waste include animal hair, meat scraps, rawhide trimmings, leather-flake chippings and trimmings, which enable thermochemical conversion and waste heat recovery [10]. However, organic contamination might occur in the thermal treatment of leather waste, due to the interactions between contained chlorine (Cl) and heavy metal [11,12]. In terms of potential organic pollutants and major air pollutants (e.g., SO_2, NO_x, etc.) from leather waste disposal, polychlorinated dibenzo-*p*-dioxins and dibenzofurans (PCDD/Fs) are the most physiologically toxic and are thereby given close attention among the trace persistent-organic-pollutants [13], which might be influenced by leather waste incineration.

PCDD/Fs include a total number of 210 kinds of isomers, consisting of 75 kinds of polychlorinated dibenzo-*p*-dioxins (PCDDs) and 135 sorts of polychlorinated dibenzofurans (PCDFs) [14]. Among them, 17 kinds of 2,3,7,8-substituted PCDD/Fs are highly toxic, and attract most attention. The biological half-life of toxic PCDD/Fs is long, ranging from 10 to 15 days for 2,3,7,8-TCDD in mice, 12 to 31 days in rats, and up to 5 to 10 years in humans [15,16]. Therefore, even one single poisoning of PCDD/Fs can persist in bodies for a long time; long-term exposure to PCDD/Fs can also lead to accumulation in bodies, which may cause serious damage [17]. PCDD/Fs are generally formed during the thermal conversion process with broad distribution, and are consequently controlled strictly by the Stockholm Convention [18]. Researchers [19,20] have elaborated well on the formation mechanism and characterization of PCDD/Fs from MSW incineration, which includes low-temperature heterogeneous synthesis (200–500 °C, and high-temperature homogeneous synthesis (500–800 °C). More specifically, low-temperature catalytic synthesis in the gas-solid phase was able to be further subdivided into precursor synthesis and de novo synthesis, and provided nearly 90% of overall PCDD/Fs during MSW treatment [21]. The forming, release and emission of PCDD/Fs during incineration are closely influenced by the source strength of Cl [22], reaction temperature [23], catalytic metal [24], and the configuration of the air-pollution control system (APCS) [25]. However, the assessment of PCDD/Fs from IW (i.e., leather waste) is still unclear, which impedes the environmental-friendly disposal of leather waste.

This study aimed to verify whether IW incineration would strengthen the emission and affect the synthesis route of PCDD/Fs. Leather waste was selected as a typical representative of IW for its large tonnage and flammability. Accordingly, the study initially evaluated and characterized the emission of 17 kinds of toxic PCDD/Fs (2,3,7,8-substitution, Table S1) and 136 kinds of tetra- through octa-chlorinated dibenzo-*p*-dioxins and dibenzofuran congeners (136 PCDD/Fs, Tables S2 and S3) from the leather-waste-incineration process in a 450 t/day fluidized-bed incinerator. The formation pathway of PCDD/Fs was also identified, based on statistical analysis. Following this, the mass flow of PCDD/Fs was assessed in both flue gas (FG) and ash, along the incineration process, including FG from the combustion chamber (CC), boiler outlet (BO), semi-dry spray neutralizer outlet (SNO), fly ash (FA) from BO, SN, and bag filter (BF), as well as bottom ash (BA). The flow and partition of PCDD/Fs at the I-TEQ level were accordingly investigated to reveal the emission characteristic of leather waste disposal.

2. Materials and Methods

2.1. Summary of the Incineration System

The trial of leather waste incineration was conducted in a 450 t/day MSW circulating fluidized incineration-system, which had the adaptability to heterogeneous fuels such as IW. As seen in Figure 1, the studied system mostly consisted of the waste pool (feeder), combustion chamber (furnace), cyclone separator, boiler for waste heat recovery, and APCS. Specifically, APCS included a semi-dry spray neutralizer (SN), active carbon injector, bag filter (BF) and chimney (i.e., bag filter outlet-BFO). The studied fluidized bed was highly adaptable to the fuel (i.e., IW), while increasing the fluidization rate and material circulation-circuit. A large amount of combusting material was brought to the upper part of the combustion chamber by the flue gas and then returned to the lower part of the furnace through internal and external circulation, which increased the share of exothermic combustion and enhanced the material exchange between the upper and lower parts of the furnace. During the trial, the system was operated steadily, to ensure dependability and steadiness. The key parameters of the incinerator and boiler were kept within a certain range near the mean values of 450 °C/5.3 MPa (main steam temperature and pressure), 60.0 t/h (main steam-output), 16.5 t/h (leather-waste input), 95% (load), 93,700 Nm^3/h (flue-gas flow rate), 890 °C (furnace outlet-temperature), 200 °C (boiler outlet-temperature), 1.5 t/h (fly-ash output) and 0.4 t/h (BA output).

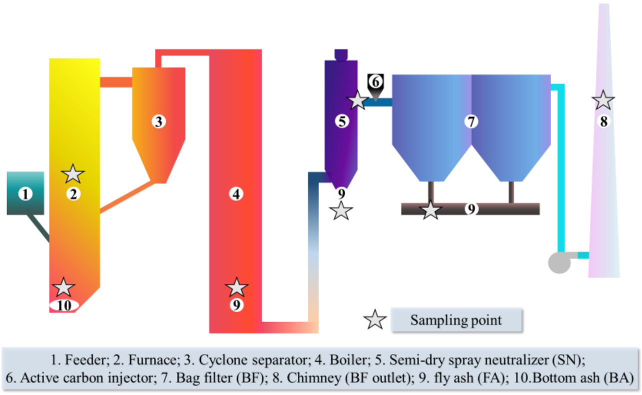

Figure 1. Schematic diagram of the studied circulating fluidized-bed-system.

2.2. Fuel Characterization

As the studied incineration system was located in the industrial park, abundant leather waste was required to be transported and disposed of in the incineration plant. The collected leather waste was typical, and representative of IW. Specifically, the leather waste was poured into and stored in a separate area of the waste pool, which was designated for the MSW. After 2–3 days' composting, leather waste was pre-treated with shearing and magnetic sorting, and then fed into the studied fluidized-bed incinerator without blended MSW. Hence, 4 samples of leather waste and 4 samples of MSW were respectively gathered and analyzed. The ultimate industrial analyses were conducted by Fuel Laboratory at Zhejiang University, following the corresponding standards CJ/T 313-2009 and CJ/T 96-2013 [26,27]. Table 1 summarizes the result, which surprisingly showed that collected leather waste had a much higher volatile fractions than MSW. This resulted in a higher low-heating-value (LHV) for IW (22,111 kJ/kg) than for MSW (6984 kJ/kg), and might raise the temperature in the combustion chamber. Moreover, a relatively higher content of chlorine in IW might further motivate PCDD/Fs formation and lift the pollutant concentrations in the FG-BO and FA.

Table 1. Composition (mean value) of MSW and IW in the incineration.

Analysis	Testing Index	IW	MSW	Units
Industrial analysis	Moisture	4.0	42.5	wt%
	Ash	8.5	17.8	wt%
	Volatile	83.9	34.0	wt%
	Fixed carbon	3.6	5.7	wt%
Ultimate analysis	C_{ar}	55.8	31.6	wt%
	H_{ar}	5.6	4.0	wt%
	N_{ar}	1.6	1.8	wt%
	S_{ar}	0.7	1.2	wt%
	O_{ar}	23.8	38.5	wt%
	Cl_{ar}	3.1	0.8	wt%
Low heating value (LHV)		22,111	6984	kJ/kg

ar represented "as the received basis".

2.3. Sampling and Analysis

FG, FA and BA samples of PCDD/Fs were collected in parallel during the leather-waste trial, following HJ 77.2-2008 and HJ 77.3-2008 [28,29]. The FG samples of PCDD/Fs were extracted by the gas sampler (ZR-3720, Junray, China) and gas analyzer (DX-4000, Gasmet, Finland) in the combustion chamber, BO, SNO and BFO (Figure 1), for 1 h at each sampling time. Moreover, FA was primarily gathered from BO, SN and BF, respectively, and then manually piled up and sealed in sample bags. In like manner, BA was sampled from the ash-discharge port of the furnace. A total number of 20 PCDD/Fs gas samples along the boiler and APCS, and 16 PCDD/Fs ash samples were extracted.

After sampling, all samples were transported to the laboratory and stored in a refrigerator below 4 °C, for further analysis. Pre-treatment and analysis of PCDD/F samples were in alignment with our previous research [30,31], referring to HJ 77.2-2008 and H J 77.3-2008 [28,29]. Detailed procedures are expanded in the Supplementary Material, in Tables S4 and S5.

2.4. Quality Assurance/Quality Control (QA/QC)

The QA/QC from the PCDD/Fs estimation was assured and evaluated as follows:

1. The sampling procedures were conducted by the technical team from the Dioxin Laboratory, Zhejiang University (China), which owns the China Inspection Body and Laboratory Mandatory Approval (CMA), and regularly participates in international laboratory comparison for the analysis of PCDD/Fs, to minimize the experimental operational errors.
2. The sampling procedures and sample pre-treatment strictly followed the national standards, which lessened the method errors to a large extent.
3. The blank test of the analysis method was carried out on approximately 10 samples for every analysis, to ensure the accuracy of the testing results of PCDD/Fs. Before using HRGC/HRMS to analyze the samples, initial precision calibration (IPR) was determined in strict accordance with the standard, and then solvent-blank and method-blank verification was carried out.

After meeting the standard requirements, the samples were pre-treated and tested for PCDD/Fs.

3. Results and Discussion

3.1. Emission of PCDD/Fs

3.1.1. Emission of 17 Kinds of Toxic PCDD/Fs

To estimate the emission of toxic PCDD/Fs (2,3,7,8-PCDD/Fs), total concentrations and I-TEQ concentrations of toxic PCDD/Fs were evaluated separately. Figure 2 provides an overview of PCDDs, PCDFs, and PCDD/Fs in gas and ash from different positions of the incineration system. What stands out in Figure 2 is the markedly lower total (or I-TEQ) concentrations of PCDD/Fs of FG from CC and FA from BO, with values of 0.087 ± 0.033 ng/Nm^3 (0.014 ± 0.004 ng I-TEQ/Nm^3) and 190.06 ± 70.38 ng/kg (13.08 ± 5.87 ng I-TEQ-Nm^3, respectively. This suggests that high-temperature synthesis of toxic PCDD/Fs could be excluded from the major contributors during leather waste incineration, which corresponds with the reported results of MSW incineration [32]. As such, toxic PCDD/Fs from BA in the furnace bottom were similarly of low intensity, with concentrations of 189.23 ± 74.25 ng/kg (11.35 ± 4.71 ng I-TEQ/kg).

There was a significant difference between PCDD/Fs concentrations of FG from BO and SNO with FG from CC, in that the former concentrations in BO and SNO reached 142.21 ± 44.57 ng/Nm^3 (17.78 ± 5.54 ng I-TEQ/Nm^3) and 116.48 ± 29.87 ng/Nm^3 (13.70 ± 4.29 ng I-TEQ/Nm^3), respectively. This phenomenon was possibly due to low-temperature heterogeneous synthesis generating massive toxic PCDD/Fs when FG flowed through the low-temperature heat-exchanger surface (i.e., the economizer) [25]. In addition to serving primarily as a purge for acidic gas (e.g., SO_2), SN also purified to some extent toxic PCDD/Fs, with a removal efficiency of 22.9%, and helped alleviate the emission of excessive toxic PCDD/Fs. Correspondingly, the gathered FA from SN showed the PCDD/Fs concentrations reaching 66.51 ± 22.52 μg/kg (2.48 ± 1.09 μg I-TEQ/kg). Therefore, it is probable that a high initial concentration of PCDD/Fs in FG-BO enriched the toxicity enhancement in FA-SN [33].

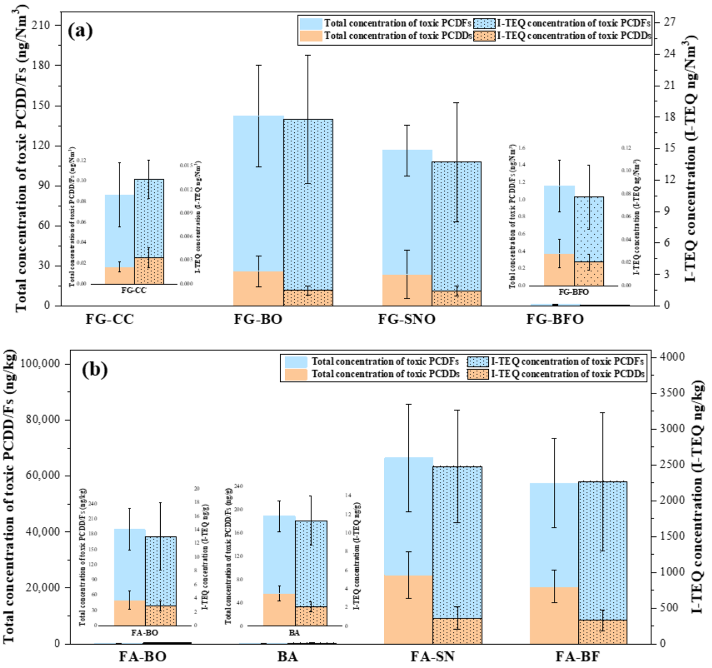

Figure 2. Total concentrations and I-TEQ concentrations of toxic PCDDs, PCDFs and PCDD/Fs in FG (**a**) and FA/BA (**b**) from the leather-waste-incineration process.

After the cleaning of the BF, toxic PCDD/Fs in FG-BFO were effectively reduced to 1.16 ± 0.33 ng/Nm^3 (0.08 ± 0.02 ng I-TEQ/Nm^3). Correspondingly, the purification efficiency of BF was calculated to be 99.4%, indicating that BF was the major purifying facility for toxic PCDD/Fs. As a result, FA-BF had PCDD/Fs contents of 57.42 ± 12.05 μg/kg (2.27 ± 0.52 μg I-TEQ/kg), which were lower than the PCDD/Fs in FA from SN. This was a rather reassuring result, since original concentrations of PCDD/Fs in the BF inlet (i.e., SNO) had already decreased, although the weight of FA in the BF was overwhelmingly higher than SN. Taken together, the emitted toxic PCDD/Fs in FG and FA/BA were lower than the limit values of 0.1 ng I-TEQ/kg and 3 μg I-TEQ/kg (GB 18485-2014 and HJ 1134-2020) [34,35]. Therefore, with the aim of contamination elimination, the toxic PCDD/Fs emission from leather waste incineration might promote a balanced and integrated enhancement of the sustainable-environment criteria.

Turning now to the distribution pattern of toxic PCDD/Fs (Figure 3), it was illustrated that notable differences between FG and FA/BA occurred both on total and I-TEQ concentration levels. The proportions of OCDD, 1,2,3,4,6,7,8-HpCDF and OCDF on the total concentration level of toxic PCDD/Fs in FA/BA were significantly higher than in FG. The possible reason was that a higher molecular mass of high chlorinated PCDD/Fs (P = 7–8) promoted a higher saturated-vapor-pressure, which facilitated a stronger adsorption of toxic PCDD/Fs in FA/BA. Further analysis of toxic PCDD/Fs on I-TEQ concentration levels revealed that 2,3,7,8-TCDD, 1,2,3,7,8-PeCDD and 1,2,3,7,8-PeCDF was dominant through 17 kinds of isomers in both FG and FA/BA. Such a result was likely to be related to the relatively higher I-TEF of the three isomers (Table S1). Additionally, similar patterns of toxic PCDD/Fs distribution were observed between FG-BO and FG-SNO, indicating that SN adsorbed toxic PCDD/Fs less selectively than BF.

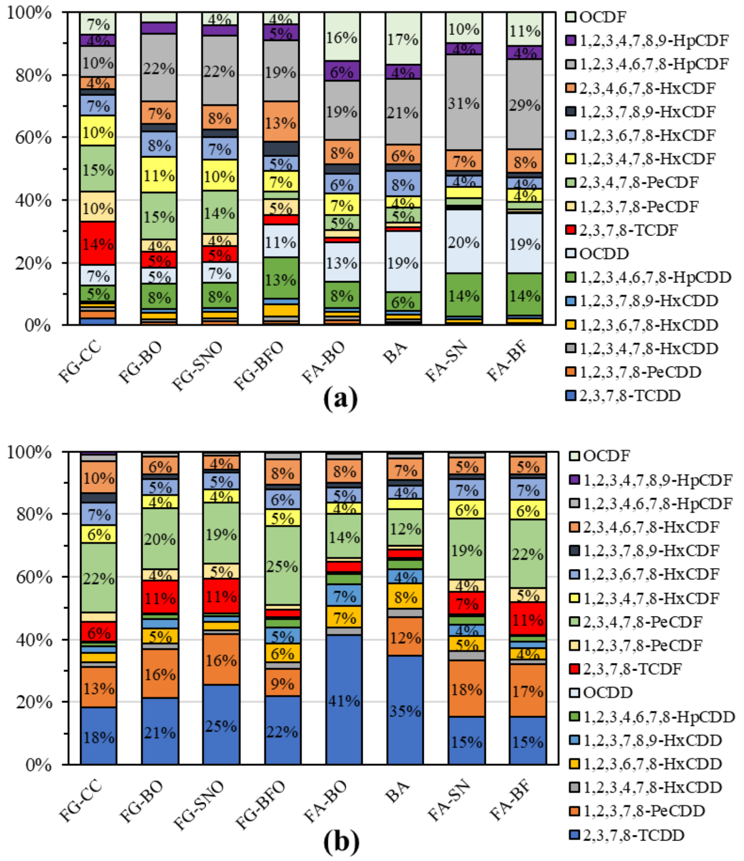

Figure 3. Distribution of 17 kinds of toxic PCDD/Fs in FG, FA and BA from leather waste incineration: (**a**) fingerprint of total toxic PCDD/Fs; (**b**) fingerprint of toxic PCDD/Fs on I-TEQ level.

3.1.2. Emission of 136 Kinds of PCDD/Fs

The results from the preliminary analysis of 136 kinds of PCDD/Fs homologues are presented in Table 2. The graph shows that there was a steep increase in the amount of PCDD/Fs in FG from BO and SNO, as well as in FA from SN and BF, compared to FG from CC and FA from BO. This trend is consistent with the trend of toxic PCDD/Fs in their corresponding medium. Concretely, the PCDD/Fs in FG from CC and FA from BO were only 1.07 ± 0.18 ng/Nm^3 and 574.12 ± 133.78 ng/kg, respectively. What is striking in this chart is the variability of the total concentrations of overall PCDD/Fs in FG from BO and FA from SN, which surprisingly reached 979.48 ± 426.67 ng/Nm^3 and 138.06 ± 37.18 µg/kg, respectively. The values were approximately 915 and 240 times higher, respectively, than the PCDD/Fs in the previous stage, and were also significantly higher than those of other MSW fluidized-bed incinerators, ranging from 93.01–366.15 ng/Nm^3 and 4.17–30.78 µg/kg, respectively [31,32]. This result might be explained by the fact that incinerated leather waste had a significantly higher Cl content than the MSW (Table 1). Higher Cl content directly enhanced the PCDD/F formation on the heat-exchanger surface and solid-fly-ash surface, while improved flue gas temperature (~260–300 °C) from leather waste combustion was most suitable for PCDD/Fs low-temperature synthesis by a related catalyst (i.e., $CuCl_2$, etc.) [21,36].

After the purification of SN and BF, emitted FG in the chimney (i.e., BFO) had a concentration of 14.83 ± 5.47 ng/Nm^3, proving the effectuality of APCS. Although 98.5% of PCDD/Fs in FG had been removed into the FA, the emitted PCDD/Fs concentration in the gas was still slightly higher than that of normal MSW incineration (0.36–7.70 ng/Nm^3) in the reported research [31,37]. Additionally, the PCDD/Fs concentration in FA from BF also reached 120.83 ± 20.21 µg/kg. Moreover, the chlorination degrees of PCDD/Fs ($d_{\text{Cl-PCDD/Fs}}$) fluctuated slightly through the FG flow, but rose from 5.68 (FA-BO) and 5.83 (BA) to 6.31 (FA-SN) and 6.29 (FA-BF), indicating further enrichment of high-chlorinated PCDD/Fs. The most obvious finding that emerged from the clusters of PCDD/Fs was that PCDD/Fs continuously increased during leather waste incineration. Even though toxic PCDD/Fs still met corresponding standards, caution is warranted when claiming that emitted values of PCDD/Fs approached the limit values. It was indicated that PCDD/Fs inhibitors and additional pollution-control devices should be adopted when incinerating combustible pure IW such as leather waste, to ensure sustainable environmental impacts in the field of pollution control.

Table 2. Total concentrations of homologues for 136 PCDD/Fs during leather waste incineration.

	FG (ng/Nm^3)				**FA**			**BA (ng/kg)**
	CC	**BO**	**SNO**	**BFO**	**BO (ng/kg)**	**SN (μg/kg)**	**BF (μg/kg)**	
TCDD	0.15 ±0.03	70.16 ±34.88	56.48 ±14.46	3.81 ±1.29	43.94 ±19.48	2.16 ±0.58	1.78 ±1.07	33.47 ±13.77
PeCDD	0.06 ±0.03	56.88 ±13.41	47.92 ±8.18	1.29 ±0.67	37.01 ±20.65	5.16 ±1.36	4.52 ±1.29	25.52 ±9.85
HxCDD	0.02 ±0.01	43.35 ±25.46	38.52 ±6.62	0.80 ±0.16	44.16 ±9.26	10.91 ±5.69	9.93 ±5.28	33.09 ±13.02
HpCDD	0.008 ±0.002	23.83 ±11.74	19.98 ±10.85	0.29 ±0.11	32.69 ±12.36	18.71 ±3.32	16.22 ±3.86	34.42 ±5.48
OCDD	0.006 ±0.002	7.32 ±3.61	7.83 ±2.82	0.12 ±0.07	24.08 ±9.91	13.59 ±2.38	10.99 ±4.68	36.85 ±15.63
TCDF	0.53 ±0.28	411.64 ±203.18	342.16 ±199.47	4.91 ±0.78	96.56 ±38.40	11.09 ±6.35	9.54 ±3.03	85.92 ±42.86
PeCDF	0.21 ±0.10	202.97 ±75.97	176.99 ±76.13	2.13 ±1.07	79.60 ±21.42	15.12 ±8.32	13.59 ±6.50	58.23 ±32.77
HxCDF	0.06 ±0.02	110.10 ±26.47	89.09 ±39.68	1.02 ±0.55	110.01 ±59.71	24.37 ±9.85	22.35 ±9.92	85.66 ±17.39
HpCDF	0.02 ±0.006	48.46 ±22.49	41.39 ±15.94	0.41 ±0.22	76.48 ±17.43	30.48 ±12.09	25.66 ±4.23	65.31 ±13.03
OCDF	0.006 ±0.003	4.76 ±1.93	4.67 ±0.87	0.05 ±0.01	29.59 ±16.82	6.47 ±1.50	6.25 ±3.10	31.74 ±18.04
Sum	1.07 ±0.18	979.48 ±426.67	825.03 ±411.00	14.83 ±5.47	574.12 ±133.78	138.06 ±37.18	120.83 ±20.21	490.22 ±191.12
$d_{\text{Cl-PCDD/Fs}}$	4.52	4.85	4.87	4.66	5.68	6.31	6.29	5.83

$d_{\text{Cl-PCDD/Fs}}$ represents the chlorination degree of 136 PCDD/Fs.

3.2. Formation Pathway of PCDD/Fs

In addition to the generation and emission of PCDD/Fs, the potential formation pathways of PCDD/Fs during leather waste incineration required further identification and validation. As mentioned above, the PCDD/Fs in FG from CC and FA from BO were much fewer than those in APCS. These results were in accordance with recent studies indicating that "3T + E" (temperature, turbulence, residue time and excessive air) adopted in an MSW incinerator maximumly reduced PCDD/Fs formed by the high-temperature synthesis in the furnace [38,39]. As a result, high-temperature synthesis (<1%) could thus be excluded from the major formation pathways of PCDD/Fs in the studied fluidized-bed incinerator.

Low-temperature catalytic synthesis contributed most of the PCDD/Fs in this case, whereas de novo synthesis or precursor synthesis will be diagnosed and determined. Figure 4 provides the summary statistics for isomer distribution on 136 PCDD/Fs. The graph shows that there are similar distribution patterns of PCDD/F homologues through the FG and FA flow sequences. Notably, 1,3,7,9- and 1,3,6,8-TCDD, 1,2,4,7,9/1,2,4,6,8- and 1,2,3,6,8-PeCDD, 1,2,3,4,6,8-HxCDD, 1,2,4,7/1,3,4,7/1,3,7,8/1,3,4,6/1,2,4,6-, 1,3,6,7/1,3,4,8/1,3,7,9/1,2,4,8- and 1,2,3,8/1,2,3,6/1,4,6,9/1,6,7,8/1,2,3,4/2,3,6,8-TCDF, 1,3,6,7,8/1,3,4,6,7/1,2,4,6,7- and 1,2,3,6,8/1,3,4,7,8/1,2,4,7,8-PeCDF are the top contributors in their corresponding homologue groups. The consistent agreement among isomer distributions of 136 PCDD/Fs implies the same formation paths.

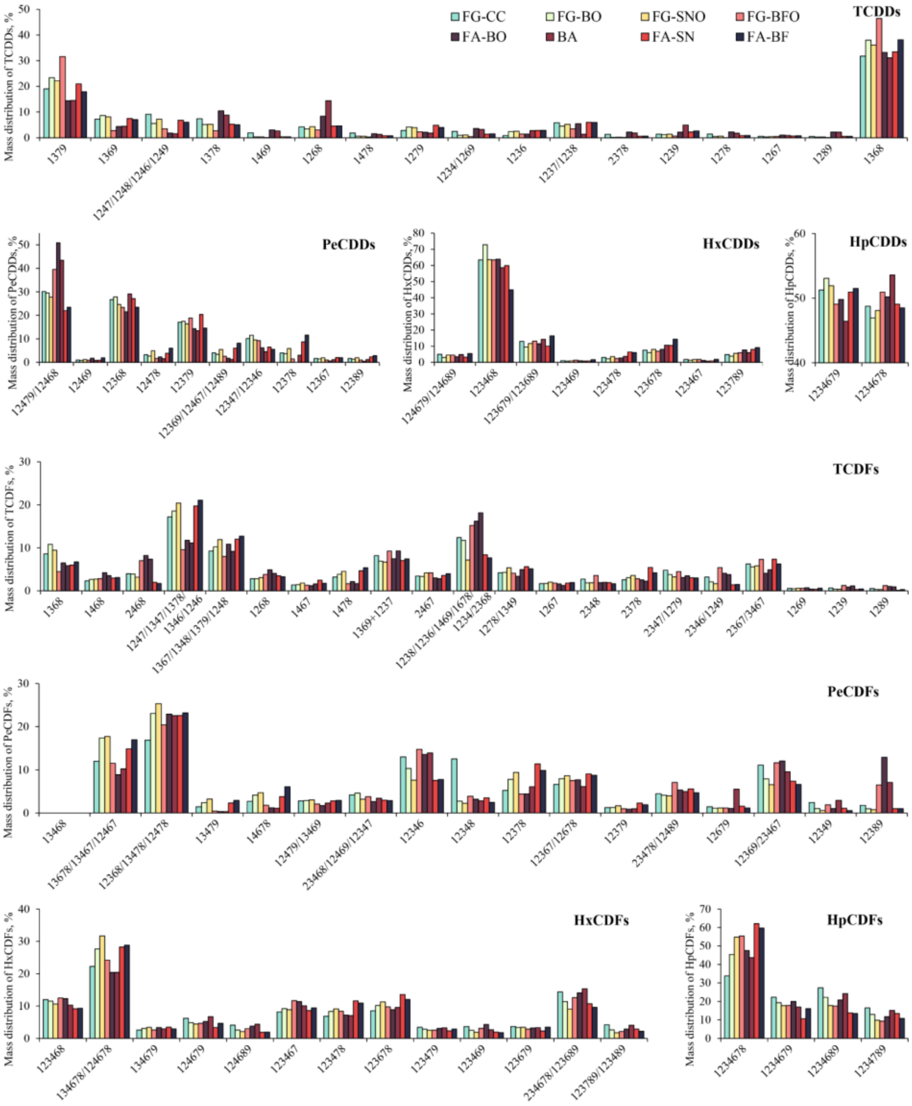

Figure 4. Distribution of 136 kinds of tetra-through octa-chlorinated PCDD/F isomers.

Chlorine-containing compounds and hydrocarbons could be oxidized and chlorinated into PCDD/Fs through de novo synthesis, in which PCDFs were generated far more than PCDDs [40]. To evaluate the proportion of de novo synthesis, the ratios of total PCDD concentrations to PCDF concentrations were calculated, and are presented in Figure 5. The most interesting aspect of this graph is the fact that the ratio of PCDDs to PCDFs is always less than 1, especially in FG from CC, BO and SNO, as well as FA/BA. This indicates that de novo synthesis is the prominent formation pathway of PCDD/Fs [21,30]. The possible reason might be that the fluidized-bed incinerator generated more FA, which contained higher contents of residue carbon brought by leather waste. Massive FA also enabled a larger reaction-surface-area for PCDD/Fs' de novo synthesis. In particular, the ratios of PCDDs to PCDFs in FG from CC, BO and SNO were 0.29, 0.26 and 0.25, respectively, whilst those in FA from BO, SN and BF were 0.46, 0.58 and 0.56, respectively. The ratio in BA was close to that in FA, with a value of 0.50, which could be generated from the high sequence-identity and similarity of BA and FA from BO. However, FG from BFO had a higher PCDDs/PCDFs ratio, of 0.74. One likely cause was that BF adsorbed more PCDFs, due to the pore structure of the coconut-shell active carbon, which was in high accordance with our previous reports [41,42].

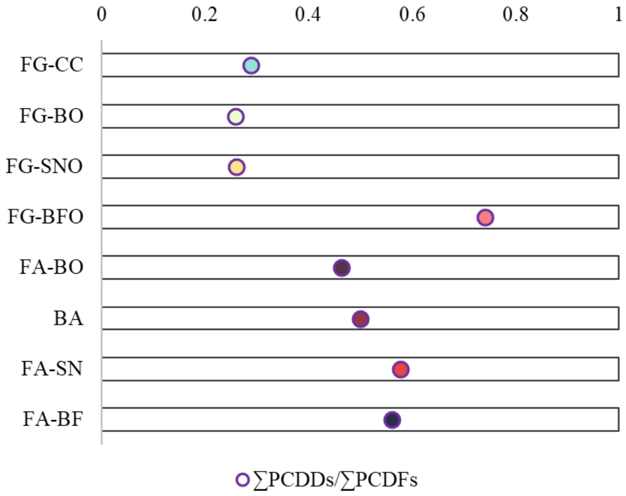

Figure 5. Ratios for total concentrations of PCDDs to PCDFs in leather waste incineration.

Precursor synthesis that condensed varied precursors such as chlorophenol (CP), dibenzodioxin (DD), dibenzofuran (DF) and other short-chain aliphatic hydrocarbons [43], was also investigated and assessed. It was widely accepted that most PCDDs in incineration were formed through precursor rearrangement (the primary role of the CP-route), while few PCDFs were generated in this way [44]. Typically, isomers of 1,3,6,8-, 1,3,7,9-TCDD, 1,2,4,6,8/1,2,4,7,9-, 1,2,3,6,8-, 1,2,3,7,9-PeCDD, 1,2,3,4,6,8-HxCDD, and 2,4,6,8-, 1,2,3,8/1,2,3,6/1,4,6,9/1,6,7,8/1,2,3,4/2,3,6,8-TCDD are treated as strongly associated CP-route congeners [45,46]. Table 3 displays the scatter diagram for the relative importance of the CP-route congeners in FG and FA/BA. It is obvious that 1,3,6,8-, 1,3,7,9-TCDD, 1,2,4,6,8/1,2,4,7,9-, 1,2,3,6,8-, 1,2,3,7,9-PeCDD and 1,2,3,4,6,8-HxCDD occupy most in their homologue group, while 2,4,6,8-, 1,2,3,8/1,2,3,6/1,4,6,9/1,6,7,8/1,2,3,4/2,3,6,8-TCDD take a small proportion. Figure 6 further illustrates the interactive correlations between CP-route congeners (e.g., 1,3,7,9- and 1,3,6,8-TCDD) and other isomers of the homologue group (e.g., 1,2,3,6-TCDD, etc.). One expected finding was the extent to which selected PCDD/F isomers merged into a cluster in the principal component analysis (PCA). The obtained gathering could be explained by the fact that potential CP-route congeners had a tight correlation with other isomers, indicating that little CP-route synthesis occurred, and still fewer synthesized with other precursors. Accordingly, precursor synthesis could also be ruled out from major formation-pathways.

Table 3. Relative importance of CP-route congeners in FG and FA/BA in leather waste incineration.

	FG (%)				**FA (%)**			**BA(%)**
	CC	**BO**	**SNO**	**BFG**	**BO**	**SN**	**BF**	
1,3,7,9-TCDD	19.1	23.4	22.1	31.6	14.4	21.0	17.9	14.5
1,3,6,8-TCDD	31.7	38.0	36.1	46.4	33.2	33.4	38.1	31.1
Sum, % of TCDDs	50.8	61.4	58.2	78.1	47.7	54.4	56.1	45.6
1,2,4,7,9/1,2,4,6,8-PeCDD	40.7	38.8	34.5	29.0	23.3	29.4	30.2	22.1
1,2,3,6,8-PeCDD	22.3	18.8	22.0	26.3	26.1	20.3	18.6	23.8
1,2,3,7,9-PeCDD	10.1	17.4	15.7	18.9	14.8	18.0	20.0	16.2
Sum, % of PeCDDs	73.1	75.0	72.2	74.2	64.3	67.7	68.7	62.2
1,2,3,4,6,8-HxCDD	47.7	52.1	48.3	65.8	44.2	45.2	47.5	39.5
2,4,6,8-TCDF	2.6	7.8	7.2	7.8	4.7	6.0	4.8	3.3
1,2,3,8/1,2,3,6/1,4,6,9/1,6,7,8/1,2,3,4/2,3,6,8-TCDF	13.7	12.3	10.8	11.4	15.7	10.5	10.8	24.2
Sum, % of TCDFs	16.3	20.1	18.0	19.2	20.4	16.6	15.6	27.5

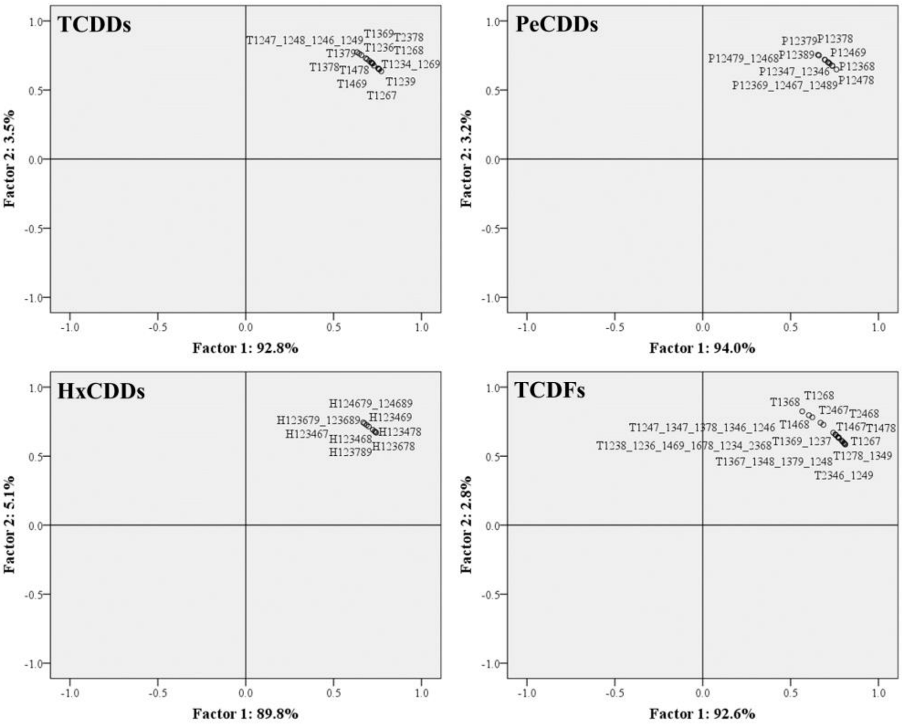

Figure 6. Principal component analysis (PCA) of CP-route congeners and the other isomers.

Since DD/DF chlorination always favored the chlorination sequence of 2→8→3→7→1 →4→6→9 positions, the 2,3,7,8-PCDD/F isomers could be discerned and pointed out as the indicators of DD/DF chlorination. For this purpose, the signal intensity of 2,3,7,8-PCDD/Fs was estimated and listed in Table 4. On the FG side, both 2,3,7,8-PCDDs and 2,3,7,8-PCDFs accounted for less than 15%, showing that little DD/DF chlorination happened in the FG. However, considerable PCDD/Fs in FA/BA were formed through DD/DF chlorination, as the fractions of 2,3,7,8-PCDDs, 2,3,7,8-PCDFs and 2,3,7,8-PCDD/Fs ranged from 27.7% to 48.2%. This evidence showed that PCDD/Fs formed by DD/DF chlorination tended to migrate into the ash, which was possibly due to the more complex structures and molecule mass of the PCDD/Fs.

Table 4. Hagenmaier profiles of 2,3,7,8-PCDD/F isomers (%) for leather waste incineration.

	FG (%)				FA (%)			BA (%)
	CC	**BO**	**SNO**	**BFO**	**BO**	**SN**	**BF**	
2,3,7,8-TCDD	1.3	0.2	0.2	0.1	2.2	0.6	0.7	1.9
1,2,3,7,8-PeCDD	3.4	2.3	2.9	0.9	5.5	2.7	2.8	5.2
1,2,3,4,7,8-HxCDD	7.0	3.2	2.7	1.9	5.0	2.4	2.6	5.2
1,2,3,6,7,8-HxCDD	6.5	6.8	6.4	5.8	6.4	7.9	8.5	9.0
1,2,3,7,8,9-HxCDD	4.2	3.6	3.5	2.5	5.6	5.3	5.5	5.9
1,2,3,4,6,7,8-HpCDD	53.8	48.4	46.7	52.7	48.3	49.0	47.9	33.1
OCDD	2.4	3.6	4.6	1.9	13.2	26.9	25.3	22.6
Sum, of PCDDs	7.0	13.0	13.8	5.9	27.7	48.7	47.3	34.8
2,3,7,8-TCDF	2.2	1.7	1.7	0.7	3.2	3.0	3.2	2.7
1,2,3,7,8-PeCDF	3.9	2.7	2.6	2.8	5.6	3.1	3.2	4.8
2,3,4,7,8-PeCDF	5.9	10.7	9.0	1.2	11.5	10.7	10.7	15.4
1,2,3,4,7,8-HxCDF	13.5	14.5	13.0	7.6	11.8	9.5	10.1	7.9
1,2,3,6,7,8-HxCDF	9.6	10.7	9.6	5.6	11.2	10.1	9.4	17.9
1,2,3,7,8,9-HxCDF	2.5	2.9	3.0	4.8	5.1	4.2	4.1	4.9
2,3,4,6,7,8-HxCDF	5.5	9.4	10.4	15.0	13.2	18.0	19.5	14.3
1,2,3,4,6,7,8-HpCDF	46.7	63.4	62.6	55.0	46.9	66.9	64.4	60.6
1,2,3,4,7,8,9-HpCDF	17.6	10.2	9.4	14.6	15.9	7.9	9.0	12.8
OCDF	0.7	0.6	0.7	0.5	7.5	7.4	8.1	9.7
Sum, of PCDFs	8.4	14.9	14.2	9.3	35.6	47.9	47.7	40.5
Sum, of PCDD/Fs	8.1	14.5	14.1	7.8	33.1	48.2	47.5	38.6

To sum up, the predominant formation pathway of PCDD/Fs in IW (i.e., leather waste) combustion in a fluidized-bed incinerator was de novo synthesis. High-temperature gaseous synthesis and precursor synthesis of PCDD/Fs could be excluded from influential formation-pathways. DD/DF chlorination also contributed to some extent.

3.3. Flow Chart of PCDD/Fs

One of the aims of this study was to evaluate and visualize the mass flow of generated PCDD/Fs (136 kinds) throughout the fluidized-bed incinerator with an APCS. Based on the key operational arguments (mentioned above), the fluxes of PCDD/Fs were expressed in units of mass per unit time, with equations as below:

$$\dot{m}_{\text{p-FG}} = c_{\text{p-FG}} \times \dot{V}_{\text{FG}} \tag{1}$$

$$\dot{m}_{\text{p-A}} = c_{\text{p-A}} \times \dot{m}_{\text{A}} \tag{2}$$

where $\dot{m}_{\text{p-FG}}$ is the mass flow rate of toxic PCDD/Fs in FG; $c_{\text{p-FG}}$ is the I-TEQ concentration of PCDD/Fs in FG; $\dot{V}_{\text{FG}}$ is the volume flow rate of FG; $\dot{m}_{\text{p-A}}$ is the mass flow rate of toxic PCDD/Fs in FA/BA; $c_{\text{p-A}}$ is the I-TEQ content of PCDD/Fs in FA; and $\dot{m}_{\text{A}}$ is the output rate of FA/BA.

The corresponding analysis of the calculated data was summarized and conceptualized in Figure 7, as indicated below. In the process, although BA and FA from BO were sampled separately, they were finally gathered together into BA and further transported out of the facility. In a similar vein, when being calculated, FA from SN and BF were also assembled and treated as a whole. Accordingly, the toxic PCDD/Fs outputs of BA and FA were 4.52 ± 1.96 μg I-TEQ/h and 3.56 ± 1.20 mg I-TEQ/h, respectively. The final output of PCDD/Fs (FG-BFO) into the atmosphere was at a relatively lower level of 7.25 ± 2.21 μg I-TEQ/h. The PCDD/Fs output into the external environment by FA was far more than the output of BA and FG. The FA of IW (leather waste) incineration was regarded as the leading contributor (>99%) to PCDD/Fs flow output, which was higher than that of MSW incineration [47]. Consequently, FA output should be addressed and handled with discretion (e.g., solidification and detoxification).

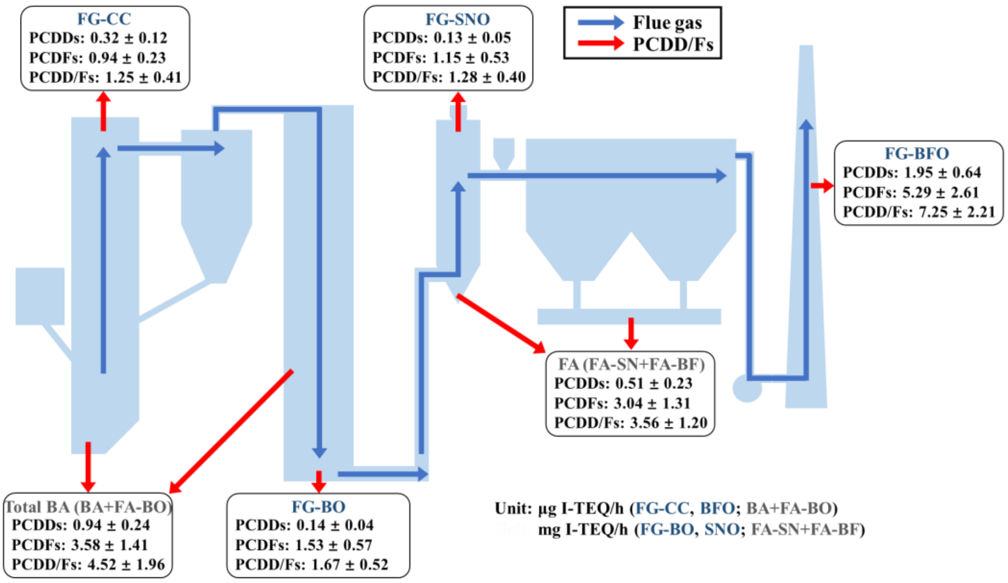

Figure 7. Flow chart of integrated PCDD/Fs on I-TEQ level.

On a closer inspection of the FG flow chart in Figure 7, we found that the FG from CC had the lowest PCDD/Fs intensity (4.52 ± 1.96 μg I-TEQ/h) in all positions. However, after the heat-exchanger surface, considerable PCDD/Fs were generated with the final mass flow rate of 1.67 ± 0.52 mg I-TEQ/h. This phenomenon was consistent with PCDD/Fs partition in MSW incineration [48,49], suggesting the obvious PCDD/Fs emission by leather waste incineration, without proper treatment technology. Afterward, SN slightly reduced PCDD/Fs in FG to 1.28 ± 0.40 mg I-TEQ/h. Nonetheless, the enriched PCDD/Fs in FA of BF was approximately two times higher than the difference between FG-SNO and FG-BFO, even though BF did adsorb PCDD/Fs into FA. The observed increase could be attributed to the FA accumulation in BF, revealing that FA of low density was in partial deposition during operation, and thus contained abnormal contents of PCDD/Fs.

Based on the above-mentioned analysis, the emission of PCDD/Fs was considerably increased and enriched into FA (>99%). Because of the long continuous-operation-time for BF, the accumulation of PCDD/Fs was observed in the emitted FA, which fortunately had less influence on FG regarding the environment. The PCDD/Fs flux on the I-TEQ level from leather waste incineration was higher than that in MSW incineration, possibly due to the source strength of Cl and the heavy metal content in IW. From the perspective of ecological sustainability, FA emitted from the studied incineration system should be properly treated by detoxification and stabilization, to avoid adding burdens to the environment.

4. Conclusions

Leather waste was selected as representative of IW in this research. The current study aimed to determine the environmental behavior (i.e., emission characteristics, formation-pathway and mass flow) of the PCDD/Fs during the IW incineration process in the fluidized-bed incinerator. Although the sample size of our study was limited, the findings were worthwhile as the first study on this topic. We believe that the obtained results will be helpful for the engineering of leather waste disposal. Specific findings are listed below.

- IW incineration might enhance the formation of 17 kinds of toxic PCDD/Fs, as well as 136 kinds of total PCDD/Fs, compared to those in MSW incineration. Specifically, the emitted toxic PCDD/Fs concentrations in FG, FA and BA were 1.16 ng/Nm^3 (0.08 ng I-TEQ/Nm^3), 57.42–66.51 μg/kg (2.27–2.48 μg I-TEQ/kg) and 189.23 ng/kg (11.35 ng I-TEQ/kg), respectively. All these values met the emission standards and were lower than the limit values of 0.1 ng I-TEQ/kg and 3 μg I-TEQ/kg (GB 18485-2014 and HJ 1134-2020). Concentrations of 136 PCDD/Fs in FG-BO, FG-BFO and FA-BF from IW incineration reached 979.48 ± 426.67 ng/Nm^3, 14.83 ± 5.47 ng/Nm^3 and 120.83 ± 20.21 μg/kg, which were higher than those of 93.01–366.15 ng/Nm^3, 0.36–7.70 ng/Nm^3 and 4.17–30.78 μg/kg in MSW incineration.
- The dominant formation-pathway during IW incineration was de novo synthesis. The fingerprints of toxic PCDD/Fs and 136 PCDD/FS in different positions of facilities were in analogous patterns, as well. Precursor synthesis (e.g., CP-route synthesis) and high-temperature gaseous synthesis of PCDD/Fs were not detected and recognized in the appropriate statistical analysis of PCDD/F isomers, and thus could be excluded. Moreover, DD/DF chlorination also contributed PCDD/Fs, which were mostly distributed in FA/BA. From the perspective of environmental sustainability, the targeted formation route of de novo synthesis should be controlled and suppressed, to eliminate potential threats to ecological environs.
- The mass flow of PCDD/Fs through the IW incineration process was comprehensively analyzed on the I-TEQ level. The results indicated that FA comprised the highest proportion (99%) of PCDD/Fs in the external environment, reaching a level of 3.56 ± 1.20 mg I-TEQ/h. De novo synthesis in low-temperature flue areas significantly strengthened the PCDD/Fs output in primary FG-BO, from 1.25 ± 0.41 μg I-TEQ/h (FG-CC) to 1.67 ± 0.52 mg I-TEQ/h (>1000 times). The accumulation of PCDD/Fs in FA was also confirmed in BF. However, with effective purification of APCS, toxic PCDD/Fs in FG were purified with a cleaning efficiency of 99.6% and emitted into the atmosphere at a discharge rate of 7.25 ± 2.21 μg I-TEQ/h. The mass fluxes of PCDD/Fs in IW incineration were higher than those in MSW incineration. The intrinsic reason for this was a higher Cl and heavy-metal content in the IW.

Supplementary Materials: The following supporting information can be downloaded at https://www.mdpi.com/article/10.3390/pr11010251/s1, Table S1: Information of 2,3,7,8-PCDD/Fs and corresponding I-TEF; Table S2: Full titles of PCDD/F homologues; Table S3: Information of 136 kinds of tetra- through octa-chlorinated dibenzo-*p*-dioxins and dibenzofuran congeners (136 PCDD/Fs); Table S4: Information of recovery standards added during pre-treatment of PCDD/Fs; Table S5: Instrumental parameters of PCDD/Fs analysis of gas chromatography/high-resolution mass spectrometry (GC/MS).

Author Contributions: Conceptualization, Y.Y. and X.L. (Xiaoqing Lin); methodology, Y.Y.; software, Y.Y.; validation, Y.Y., X.W. and W.S.; formal analysis, Y.Y.; investigation, Y.Y.; resources, Y.M., H.Y., W.H. and L.Z.; data curation, Y.Y.; writing—original draft preparation, Y.Y.; writing—review and editing, Y.Y., X.L. (Xiaoqing Lin) and X.L. (Xiaodong Li); visualization, Y.Y. and X.W.; supervision, X.L. (Xiaodong Li) and S.L.; project administration, X.L. (Xiaoqing Lin); funding acquisition, X.L. (Xiaodong Li). All authors have read and agreed to the published version of the manuscript.

Funding: This research was supported by "the Fundamental Research Funds for the Central Universities (K20220145)", and "the Science and Technology Project of China Huaneng Group Co., Ltd. (HNKJ20-H62)".

Institutional Review Board Statement: Not applicable.

Informed Consent Statement: Not applicable.

Data Availability Statement: The data will be available when requested.

Acknowledgments: I would like to extend my thanks to Yixin Wang and Mingjun Gao, for language support.

Conflicts of Interest: The authors declare no conflict of interest.

References

1. NBSC. *China Statistical Yearbook 2021*; National Bureau of Statistics of China: Beijing, China, 2021.
2. NBSC. *China Statistical Yearbook 2011*; National Bureau of Statistics of China: Beijing, China, 2011.
3. Tian, G.; Xia, Q.; Wu, Z.; Fu, T. Ecological network analysis of industrial wastes metabolism based on input-output model for Jiangsu, China. *Waste Manag.* **2022**, *143*, 23–34. [CrossRef] [PubMed]
4. Vkga, B.; Ps, C.; Rs, D.; Mka, E.; Cgd, F.; Apg, H. Assessing the impact of industrial waste on environment and mitigation strategies: A comprehensive review. *J. Hazard. Mater.* **2020**, *398*, 123019.
5. Otakulov, B.A.; Abdullayev, I.A.; Sultonov, K.S.O. Raw material base of construction materials and use of industrial waste. *Sci. Prog.* **2021**, *2*, 1609–1612.
6. Boltakova, N.; Faseeva, G.; Kabirov, R.; Nafikov, R.; Zakharov, Y.A. Utilization of inorganic industrial wastes in producing construction ceramics. Review of Russian experience for the years 2000–2015. *Waste Manag.* **2017**, *60*, 230–246. [CrossRef]
7. Goli, V.; Singh, D.N.; Baser, T. A critical review on thermal treatment technologies of combustible fractions from mechanical biological treatment plants. *J. Environ. Chem. Eng.* **2021**, *9*, 105643. [CrossRef]
8. Jin, C.; Sun, S.; Yang, D.; Sheng, W.; Ma, Y.; He, W.; Li, G. Anaerobic digestion: An alternative resource treatment option for food waste in China. *Sci. Total Environ.* **2021**, *779*, 146397. [CrossRef]
9. Ge, S.; Wang, Q.; Diao, S.; Wang, X.; Yuan, Y.; Luan, J. Research progress and application of solid leather waste. *Leather Chem.* **2019**, *36*, 37–42.
10. Li, Y.; Guo, R.; Lu, W.; Zhu, D. Research progress on resource utilization of leather solid waste. *J. Leather Sci. Eng.* **2019**, *1*, 6. [CrossRef]
11. Viczek, S.A.; Aldrian, A.; Pomberger, R.; Sarc, R. Origins and carriers of Sb, As, Cd, Cl, Cr, Co, Pb, Hg, and Ni in mixed solid waste–a literature-based evaluation. *Waste Manag.* **2020**, *103*, 87–112. [CrossRef]
12. Dudyński, M.; Dudyński, K.; Kluska, J.; Ochnio, M.; Kazimierski, P.; Kardaś, D. Gasification of leather waste for energy production: Laboratory scale and industrial tests. *Int. J. Energy Res.* **2021**, *45*, 18540–18553. [CrossRef]
13. Zhan, M.; Sun, C.; Chen, T.; Li, X. Emission characteristics for co-combustion of leather wastes, sewage sludge, and coal in a laboratory-scale entrained flow tube furnace. *Environ. Sci. Pollut. Res.* **2019**, *26*, 9707–9716. [CrossRef]
14. Zhu, F.; Li, X.; Lu, J.-W.; Hai, J.; Zhang, J.; Xie, B.; Hong, C. Emission characteristics of PCDD/Fs in stack gas from municipal solid waste incineration plants in Northern China. *Chemosphere* **2018**, *200*, 23–29. [CrossRef] [PubMed]
15. Tuomisto, J. Dioxins and dioxin-like compounds: Toxicity in humans and animals, sources, and behaviour in the environment. *WikiJournal Med.* **2019**, *6*, 8. [CrossRef]
16. Yoshioka, W.; Tohyama, C. Mechanisms of developmental toxicity of dioxins and related compounds. *Int. J. Mol. Sci.* **2019**, *20*, 617. [CrossRef]

17. Cheruiyot, N.K.; Lee, W.-J.; Yan, P.; Mwangi, J.K.; Wang, L.-C.; Gao, X.; Lin, N.-H.; Chang-Chien, G.-P. An overview of PCDD/F inventories and emission factors from stationary and mobile sources: What we know and what is missing. *Aerosol Air Qual. Res.* **2016**, *16*, 2965–2988. [CrossRef]
18. Fiedler, H.; van der Veen, I.; de Boer, J. Interlaboratory assessments for dioxin-like POPs (2016/2017 and 2018/2019). *Chemosphere* **2022**, *288*, 132449. [CrossRef] [PubMed]
19. Yang, L.; Liu, G.; Shen, J.; Wang, M.; Yang, Q.; Zheng, M. Environmental characteristics and formations of polybrominated dibenzo-p-dioxins and dibenzofurans. *Environ. Int.* **2021**, *152*, 106450. [CrossRef] [PubMed]
20. Peng, Y.; Lu, S.; Li, X.; Yan, J.; Cen, K. Formation, measurement, and control of dioxins from the incineration of municipal solid wastes: Recent advances and perspectives. *Energy Fuels* **2020**, *34*, 13247–13267. [CrossRef]
21. Zhang, M.; Buekens, A. De novo synthesis of dioxins: A review. *Int. J. Environ. Pollut.* **2016**, *60*, 63–110. [CrossRef]
22. Zhang, M.; Fujimori, T.; Shiota, K.; Li, X.; Takaoka, M. Formation pathways of polychlorinated dibenzo-p-dioxins and dibenzofurans from burning simulated PVC-coated cable wires. *Chemosphere* **2021**, *264*, 128542. [CrossRef]
23. Lin, X.; Wang, X.; Ying, Y.; Wu, A.; Chen, Z.; Wang, L.; Yu, H.; Zhang, H.; Ruan, A.; Li, X. Formation pathways, gas-solid partitioning, and reaction kinetics of PCDD/Fs associated with baghouse filters operated at high temperatures: A case study. *Sci. Total Environ.* **2023**, *857*, 159551. [CrossRef]
24. Zhang, M.; Fujimori, T.; Shiota, K.; Buekens, A.; Mukai, K.; Niwa, Y.; Li, X.; Takaoka, M. Thermochemical formation of dioxins promoted by chromium chloride: In situ Cr-and Cl-XAFS analysis. *J. Hazard. Mater.* **2020**, *388*, 122064. [CrossRef] [PubMed]
25. Lin, X.Q.; Ma, Y.F.; Chen, Z.L.; Li, X.D.; Lu, S.Y.; Yan, J.H. Effect of different air pollution control devices on the gas/solid-phase distribution of PCDD/F in a full-scale municipal solid waste incinerator. *Environ. Pollut.* **2020**, *265*, 114888. [CrossRef]
26. *CJ/T 313-2009*; Sampling and Analysis Methods for Domestic Waste. Ministry of Housing and Urban-Rural Development of the People's Republic of China: Beijing, China, 2009.
27. *CJ/T 96-2013*; General Detecting Methods for the Chemical Characteristic of Domestic Refuse. Ministry of Housing and Urban-Rural Development of the People's Republic of China: Beijing, China, 2013.
28. *HJ 77.2-2008*; Ambient Air and Flue Gas-Determination of Polychlorinated Dibenzo-p-Dioxins (PCDDs) and Polychlorinated Dibenzofurans (PCDFs) Isotope Dilution HRGC-HRMS. Ministry of Environmental Protection of the People's Republic of China: Beijing, China, 2008.
29. *HJ 77.3-2008*; Solid Waste-Determination of Polychlorinated Dibenzo-p-Dioxins (PCDDs) and Polychlorinated Dibenzofurans (PCDFs) Isotope Dilution HRGC-HRMS. Ministry of Environmental Protection of the People's Republic of China: Beijing, China, 2008.
30. Ying, Y.; Ma, Y.; Li, X.; Lin, X. Emission characteristics and formation pathways of PCDD/Fs from cocombustion of municipal solid waste in a large-scale coal-fired power plant. *Energy Fuels* **2021**, *35*, 8221–8233. [CrossRef]
31. Ying, Y.; Xu, L.; Lin, X.; Zhang, H.; Li, X.; Lu, S.; Cao, Y.; Long, J. Influence of different kinds of incinerators on PCDD/Fs: A case study of emission and formation pathway. *Environ. Sci. Pollut. Res.* **2022**. *online ahead of print*. [CrossRef] [PubMed]
32. Zhang, M.; Yang, J.; Buekens, A.; Olie, K.; Li, X. PCDD/F catalysis by metal chlorides and oxides. *Chemosphere* **2016**, *159*, 536–544. [CrossRef] [PubMed]
33. Zhou, Y.; Liu, J. Emissions, environmental levels, sources, formation pathways, and analysis of polybrominated dibenzo-p-dioxins and dibenzofurans: A review. *Environ. Sci. Pollut. Res.* **2018**, *25*, 33082–33102. [CrossRef]
34. *GB 18485-2014*; Standard for Pollution Control on the Municipal Solid Waste Incineration. Ministry of Ecology and Environment of the People's Republic of China: Beijing, China, 2014.
35. *HJ 1134-2020*; Technical Specification for Pollution Control of Fly-Ash from Municipal Solid Waste Incineration. Ministry of Ecology and Environment of the People's Republic of China: Beijing, China, 2020.
36. Zhang, M.; Buekens, A.; Ma, S.; Li, X. Iron chloride catalysed PCDD/F-formation: Experiments and PCDD/F-signatures. *Chemosphere* **2018**, *191*, 72–80. [CrossRef]
37. Ma, Y.; Lin, X.; Chen, Z.; Li, X.; Lu, S.; Yan, J. Influence factors and mass balance of memory effect on PCDD/F emissions from the full-scale municipal solid waste incineration in China. *Chemosphere* **2020**, *239*, 124614. [CrossRef]
38. Zhang, G.; Hai, J.; Cheng, J. Characterization and mass balance of dioxin from a large-scale municipal solid waste incinerator in China. *Waste Manag.* **2012**, *32*, 1156–1162. [CrossRef] [PubMed]
39. Zhou, H.; Meng, A.; Long, Y.; Li, Q.; Zhang, Y. A review of dioxin-related substances during municipal solid waste incineration. *Waste Manag.* **2015**, *36*, 106–118. [CrossRef] [PubMed]
40. Chen, Z.; Lin, X.; Lu, S.; Li, X.; Yan, J. Suppressing formation pathway of PCDD/Fs by SN-containing compound in full-scale municipal solid waste incinerators. *Chem. Eng. J.* **2019**, *359*, 1391–1399. [CrossRef]
41. Wang, P.; Lin, X.; Xu, S.; Li, X.; Ma, Y.; Liu, W.; Wu, J.; Ding, J. Simultaneous removal of PCDD/Fs and mercury by activated carbon from a full-scale MSW incinerator in southeast China. *Environ. Sci. Pollut. Res.* **2022**. *online ahead of print*. [CrossRef]
42. Guo, X.; Wang, P.; Ma, Y.; Lin, X.; Li, X. Experimental study on the effect of activated carbon pore parameters on dioxin gas-phase adsorption. *Environ. Sanit. Eng.* **2020**, *28*, 52–56.
43. Wang, D.; Zhang, H.; Ren, M.; Fan, Y.; Gao, Y.; Lv, Z.Y.; Yu, Y.; Chen, J. Electrophilic chlorination of dibenzo-p-dioxin and dibenzofuran over composite copper and iron chlorides and oxides in combustion flue gas. *Chemosphere* **2020**, *256*, 127065. [CrossRef]
44. Yang, L.; Liu, G.; Zheng, M.; Zhao, Y.; Jin, R.; Wu, X.; Xu, Y. Molecular mechanism of dioxin formation from chlorophenol based on electron paramagnetic resonance spectroscopy. *Environ. Sci. Technol.* **2017**, *51*, 4999–5007. [CrossRef]

45. Shi, X.; Zhang, R.; Zhang, H.; Xu, F.; Zhang, Q.; Wang, W. Influence of water on the homogeneous gas-phase formation mechanism of polyhalogenated dioxins/furans from chlorinated/brominated phenols as precursors. *Chemosphere* **2015**, *137*, 142–148. [CrossRef]
46. Wang, X.; Chen, J.; Ni, Y. Polychlorinated dibenzo-p-dioxin and dibenzofuran precursors and formation mechanisms during non-woodpulp chlorine bleaching process. *Chemosphere* **2018**, *211*, 1–9. [CrossRef]
47. Ren, M.; Lv, Z.Y.; Xu, L.; Lu, Q.; Zhang, X.; Yu, Y.; Fan, Y.; Gao, Y.; Chen, J.; Zhang, H. Partitioning and removal behaviors of PCDD/Fs, PCBs and PCNs in a modern municipal solid waste incineration system. *Sci. Total Environ.* **2020**, *735*, 139134. [CrossRef]
48. Cai, J.; Zhong, R.; Liu, X.; Liu, Q.; Wu, H.; Yan, F.; Huang, J.; Zhang, Z. Effects of evaporation capacity on the formation and removal of PCDD/Fs in a full-scale municipal solid waste incinerator. *Process Saf. Environ. Prot.* **2021**, *154*, 18–31. [CrossRef]
49. Huang, Y.; Lu, J.-W.; Xie, Y.; Hong, C.; Shi, L.; Hai, J. Process tracing of PCDD/Fs from economizer to APCDs during solid waste incineration: Re-formation and transformation mechanisms. *Waste Manag.* **2021**, *120*, 839–847. [CrossRef] [PubMed]